

Synthesis and Structures of Novel Zerovalent Ruthenium *p*-Quinone Complexes and a Bimetallic *p*-Biquinone Complex

Yasuyuki Ura, Yoshitaka Sato, Masashi Shiotsuki, Toshiaki Suzuki, Kenji Wada, Teruyuki Kondo, and Take-aki Mitsudo*

Department of Energy and Hydrocarbon Chemistry, Graduate School of Engineering, Kyoto University, Sakyo-ku, Kyoto 606-8501, Japan

Received September 4, 2002

$\text{Ru}(\eta^6\text{-cot})(\eta^2\text{-dmfm})_2$ (**1**; cot = 1,3,5-cyclooctatriene, dmfm = dimethyl fumarate) reacted with *p*-quinones to give novel *p*-quinone-coordinated ruthenium(0) complexes, $\text{Ru}(\eta^6\text{-cot})$ -(*p*-quinone) (**2**), in good to high yields via the replacement of two dimethyl fumarates by *p*-quinones. The reaction of **1** with *p*-biquinone gave a novel bimetallic zerovalent complex $\{\text{Ru}(\eta^6\text{-cot})\}_2(\textit{p}\text{-biquinone})$ (**3**), in which *p*-biquinone coordinates to two isolated “Ru(cot)” moieties with a unique mode and the two Ru(cot) groups are located at endo positions. Complexes **2** and **3** have either *p*-quinone or *p*-biquinone as π -acceptor ligands. The structures of complexes $\text{Ru}(\eta^6\text{-cot})(2,6\text{-dimethoxy-}p\text{-quinone})$ (**2f**) and **3** were determined by X-ray crystallography.

Introduction

Among low-valent transition-metal complexes bearing an olefinic π -acceptor ligand, *p*-quinone complexes have been intensively investigated.^{1–22} The study of *p*-quinone ligands is intriguing not only because of their role

in proton/electron transfer but also in view of their strong electron-accepting ability through π -back-donation. Since the degree of π -acidity can be controlled by changing the substituents on quinone, the electron density on the metal center is easily adjusted, which is important from the viewpoint of catalytic activity. The first synthesis of a transition-metal *p*-quinone complex, $\text{Fe}(\text{CO})_3(\text{duroquinone})$, was accomplished by Sternberg, Markby, and Wender in 1958.¹ Several group 9 and 10 metal *p*-quinone complexes have been reported so far.^{2–16} In contrast, there are very few examples of other metal complexes such as iron(0),^{1,17} ruthenium(II),¹⁸ manganese(–I),¹⁹ and molybdenum(II).²⁰

The methods used to prepare *p*-quinone complexes can be divided into four classes: (1) direct ligand exchange of appropriate complexes with *p*-quinones (method A), (2) coupling of alkynes with carbon monoxides on the transition-metal (method B), (3) reaction of maleoyl/phthaloylmethyl species with an alkyne (method C), and (4) deprotonation of hydroquinone complexes (method D). In the synthesis of *p*-quinone complexes by method A, duroquinone has been frequently used,^{2–5,7,9,11} whereas few examples of other *p*-quinone complexes have been reported.^{10,12,13,16} $\text{Fe}(\text{CO})_3(\text{duroquinone})$,¹ $\text{Cp-Co}(p\text{-quinone})$,⁸ and $\text{CpMoCl}(\text{CO})(\text{duroquinone})$ ²⁰ have been prepared by method B. Liebeskind and co-workers reported a high-yield synthesis of *p*-quinone cobalt complexes through method C, in which maleoyl/phthaloylmethyl species were generated by oxidative addition

(1) Sternberg, H. W.; Markby, R.; Wender, I. *J. Am. Chem. Soc.* **1958**, *80*, 1009.

(2) (a) Schrauzer, G. N.; Thyret, H. *J. Am. Chem. Soc.* **1960**, *82*, 6420. (b) Schrauzer, G. N.; Thyret, H. *Z. Naturforsch.* **1961**, *16b*, 353. (c) Schrauzer, G. N.; Thyret, H. *Z. Naturforsch.* **1962**, *17b*, 73. (d) Schrauzer, G. N.; Thyret, H. *Angew. Chem., Int. Ed. Engl.* **1963**, *2*, 478.

(3) Schrauzer, G. N.; Dewhirst, K. C. *J. Am. Chem. Soc.* **1964**, *86*, 3265.

(4) Glick, M. D.; Dahl, L. F. *J. Organomet. Chem.* **1965**, *3*, 200.

(5) (a) Aleksandrov, G. G.; Gusev, A. I.; Khandkarova, V. S.; Struchkov, Yu. T.; Gubin, S. P. *Chem. Commun.* **1969**, 748. (b) Aleksandrov, G. G.; Struchkov, Yu. T.; Khandkarova, V. S.; Gubin, S. P. *J. Organomet. Chem.* **1970**, *25*, 243.

(6) Uchtman, V. A.; Dahl, L. F. *J. Organomet. Chem.* **1972**, *40*, 403.

(7) Slocum, D. W.; Engelmann, T. R. *J. Am. Chem. Soc.* **1972**, *94*, 8596.

(8) (a) Dickson, R. S.; Kirsch, H. P. *Aust. J. Chem.* **1974**, *27*, 61. (b) Dickson, R. S.; Johnson, S. H. *Aust. J. Chem.* **1976**, *29*, 2189. (c) Corrigan, P. A.; Dickson, R. S. *Aust. J. Chem.* **1981**, *34*, 1401.

(9) Bodner, G. M.; Engelmann, T. R. *J. Organomet. Chem.* **1975**, *88*, 391.

(10) Minematsu, H.; Takahashi, S.; Hagihara, N. *J. Organomet. Chem.* **1975**, *91*, 389.

(11) (a) Fairhurst, G.; White, C. *J. Organomet. Chem.* **1978**, *160*, C17. (b) Fairhurst, G.; White, C. *J. Chem. Soc., Dalton Trans.* **1979**, 1531.

(12) (a) Chetcuti, M. J.; Howard, J. A. K.; Pfeffer, M.; Spencer, J. L.; Stone, F. G. A. *J. Chem. Soc., Dalton Trans.* **1981**, 276. (b) Chetcuti, M. J.; Herbert, J. A.; Howard, J. A. K.; Pfeffer, M.; Spencer, J. L.; Stone, F. G. A.; Woodward, P. *J. Chem. Soc., Dalton Trans.* **1981**, 284.

(13) Hiramatsu, M.; Shiozaki, K.; Fujinami, T.; Sakai, S. *J. Organomet. Chem.* **1983**, *246*, 203.

(14) (a) Jewell, C. F., Jr.; Liebeskind, L. S.; Williamson, M. *J. Am. Chem. Soc.* **1985**, *107*, 6715. (b) Liebeskind, L. S.; Jewell, C. F., Jr. *J. Organomet. Chem.* **1985**, *285*, 305. (c) Cho, S. H.; Wirtz, K. R.; Liebeskind, L. S. *Organometallics* **1990**, *9*, 3067.

(15) Le Bras, J.; Amouri, H.; Vaissermann, J. *Organometallics* **1998**, *17*, 1116.

(16) Klein, H.-F.; Auer, E.; Dal, A.; Lemke, U.; Lemke, M.; Jung, T.; Rohr, C.; Florke, U.; Haupt, H.-J. *Inorg. Chim. Acta* **1999**, *287*, 167.

(17) Cooke, J.; Takats, J. *J. Am. Chem. Soc.* **1997**, *119*, 11088.

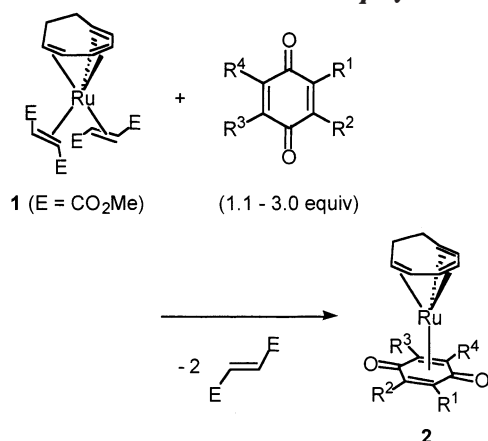
(18) Rosete, R. O.; Cole-Hamilton, D. J.; Wilkinson, G. *J. Chem. Soc., Dalton Trans.* **1979**, 1618.

(19) (a) Oh, M.; Carpenter, G. B.; Sweigart, D. A. *Angew. Chem., Int. Ed.* **2001**, *40*, 3191. (b) Oh, M.; Carpenter, G. B.; Sweigart, D. A. *Organometallics* **2002**, *21*, 1290.

(20) Davidson, J. L.; Green, M.; Stone, F. G. A.; Welch, A. J. *J. Chem. Soc., Dalton Trans.* **1976**, 738.

(21) Le Bras, J.; Amouri, H.; Vaissermann, J. *J. Organomet. Chem.* **1998**, *553*, 483.

(22) Sun, S.; Carpenter, G. B.; Sweigart, D. A. *J. Organomet. Chem.* **1996**, *512*, 257.

Table 1. Reactions of 1 with *p*-Quinones

entry	R ¹	R ²	R ³	R ⁴	amount of quinone (equiv)	solvent	reaction condition	product	yield (%) ^a
1	H	H	H	H	1.1	Et ₂ O	rt, 2 h	2a	98
2	Me	H	H	H	1.1	Et ₂ O	reflux, 4 h	2b	87
3	Me	H	H	Me	2.2	Et ₂ O	reflux, 4 h	2c	94
4	Ph	H	Ph	H	1.2	Et ₂ O	reflux, 4 h	2d	64
5	Cl	H	Cl	H	1.1	Et ₂ O	reflux, 4 h	2e	65
6	OMe	H	H	OMe	1.1	toluene	80 °C, 2 h	2f	60
7	-CH=CH- CH=CH-	H	H	H	3.0	Et ₂ O	reflux, 4 h	2g	89

^a Isolated yield.

of cyclobutenedione or benzocyclobutenedione to a low-valent cobalt complex.¹⁴ Iridium and manganese η^6 -hydroquinone complexes have been prepared by Amouri and co-workers^{15,21} and Sweigart and co-workers,^{19,22} respectively, taking advantage of method D; η^5 -semi-quinone and η^4 -*p*-quinone complexes are synthesized.

Recently, we reported a novel zerovalent ruthenium complex Ru(η^6 -cot)(dmfm)₂ (**1**; η^6 -cot = 1-6- η -cyclooctatriene, dmfm = dimethyl fumarate).²³ Complex **1** was found to be an excellent catalyst for a unique dimerization of 2,5-norbornadiene to afford a novel half-cage compound.²³ In this catalyst, the coordinated dimethyl fumarate was found to be crucial as a π -acceptor ligand. Complex **1** is also a versatile precursor for novel Ru(0) complexes, as we demonstrated previously.²⁴ In the course of our further investigation of the reactivity of **1**, we found that reactions with various *p*-quinones and

a *p*-biquinone under mild conditions give novel complexes Ru(η^6 -cot)(*p*-quinone) (**2**) and {Ru(η^6 -cot)}₂(*p*-biquinone) (**3**) in high yields via simple and selective ligand exchange (method A) between π -acceptors. We report here the synthesis and structures of a series of novel *p*-quinone ruthenium(0) complexes **2** and a unique *p*-biquinone bimetallic complex **3**.

Results and Discussion

Ru(η^6 -cot)(*p*-quinone) (2**).** As shown in Table 1, the reactions of **1** with *p*-quinones were performed in Et₂O at room temperature for 2 h (entry 1), under reflux for 4 h (entries 2–5, 7), and in toluene at 80 °C for 2 h (entry 6), respectively. The selective ligand exchange between π -acceptors, dimethyl fumarate and *p*-quinone, proceeded smoothly to afford **2** in good to high yield. Several kinds of *p*-quinones with an electron-donating group (entries 2, 3, 6) or an electron-withdrawing group (entries 4, 5) were found to be suitable for this substitution reaction, including *p*-naphthoquinone (entry 7). The reaction with chloranil (tetrachloro-*p*-benzoquinone) also proceeded to give a precipitate; however, spectroscopic characterization was impossible because of the low solubility of the product. The use of DDQ (2,3-dichloro-5,6-dicyano-*p*-benzoquinone) gave a complex mixture of products.

The structures of **2a–2g** were deduced on the basis of ¹H and ¹³C NMR, IR, and mass spectra. The ¹H and ¹³C NMR data for **2a–2g** are summarized in Tables 2 and 3, respectively. In the ¹H NMR spectra of **2**, the signals for the olefinic protons of the 1,3,5-cyclooctatriene moiety appear at 6.6–4.1 ppm, and those for the methylene protons appear at 2.8–0.1 ppm. The signals for the olefinic protons of *p*-quinone ligands in **2** appear at 5.0–5.8 ppm, which are shifted to a higher magnetic field than those of the corresponding free *p*-quinones by 1.5–1.8 ppm. The appearance of these signals as singlet peaks, except in **2b**, suggests that cyclooctatriene rotates freely on ruthenium at room temperature in solution. In the ¹³C NMR spectra of **2**, the carbonyl carbons of the coordinated *p*-quinones are observed at 153–159 ppm, which are shifted upfield by ca. 30 ppm compared with free *p*-quinones, whereas one

Table 2. ¹H NMR Data of 2a–2g (δ , ppm)^a

complex	<i>p</i> -quinone		1,3,5-cyclooctatriene
	=CH	others	
2a	5.02 (s, 4H)		6.33 (m, 2H), 5.56 (br t, 6.8, 2H), 5.04 (m, 2H), 2.22 (m, 2H), 1.00 (m, 2H)
2b	5.16 (s, 1H), 5.00 (m, 2H)	1.82 (s, 3H)	6.20 (m, 2H), 5.42 (br t, 7.4, 1H), 5.38 (br t, 7.4, 1H), 4.90 (m, 2H), 2.19 (m, 2H), 0.95 (m, 2H)
2c	5.09 (s, 2H)	1.82 (s, 6H)	6.04 (dd, 4.9, 2.0, 2H), 5.22 (ddd, 8.3, 4.9, 2.0, 2H), 4.74 (m, 2H), 2.14 (m, 2H), 0.90 (m, 2H)
2d	5.59 (s, 2H)	7.36–7.84 (m, 10H)	5.96 (t, 7.3, 1H), 5.61 (m, 1H), 5.50 (t, 8.0, 1H), 5.35 (t, 8.5, 1H), 5.03 (m, 1H), 4.12 (dd, 13.6, 7.4, 1H), 2.29 (m, 1H), 1.53 (m, 2H), 0.09 (m, 1H)
2e	5.76 (s, 2H)		6.58 (t, 7.4, 1H), 6.19 (t, 8.3, 1H), 5.31 (t, 7.1, 2H), 4.90 (t, 8.8, 1H), 4.80 (dd, 8.0, 14.4, 1H), 2.75 (m, 1H), 1.91 (m, 2H), 0.20 (m, 1H)
2f	5.24 (s, 2H)	3.68 (s, 6H)	6.13 (m, 2H), 5.27 (m, 2H), 4.91 (m, 2H), 2.17 (m, 2H), 0.89 (m, 2H)
2g	5.20 (s, 2H)	8.01 (m, 2H), 7.40 (m, 2H)	5.39 (m, 2H), 4.92 (m, 2H), 4.79 (m, 2H), 1.97 (m, 2H), 0.57 (m, 2H)

^a Measured in CDCl₃ at room temperature and 400 MHz. s = singlet, d = doublet, t = triplet, m = multiplet, br = broad. Figures in parentheses are the values of the coupling constants, J_{H-H} (in Hz).

Table 3. ^{13}C NMR Data of **2a–2g** (δ , ppm)^a

complex	<i>p</i> -quinone			1,3,5-cyclooctatriene
	C=C (coordinated)	C=O	others	
2a	83.7	158.6		99.8, 92.6, 91.1, 32.9
2b	99.7, 87.2, 82.4, 82.3	158.1, 157.6	15.7	99.9, 99.7, 94.3, 93.2, 91.8, 90.6, 32.9, 32.6
2c	97.8, 85.7	158.0, 156.8	15.7	99.9, 94.8, 90.8, 32.6
2d	97.7, 81.8	158.6	133.0, 128.8, 128.6, 128.3	102.4, 101.9, 97.7, 95.8, 93.2, 87.7, 34.4, 29.7
2e	103.1, 82.7	154.2		101.5, 101.4, 100.9, 100.8, 98.3, 90.8, 37.6, 28.6
2f	132.3, 68.6	153.4, 141.3	56.4	99.1, 94.7, 91.0, 32.8
2g	109.9, 74.3	157.0	130.2, 125.2	101.8, 95.5, 87.4, 32.0

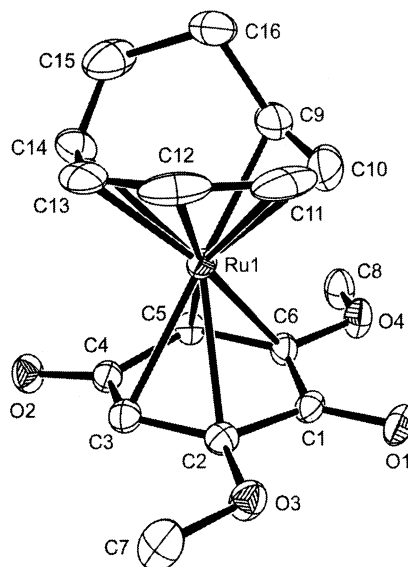
^a Measured in CDCl_3 at room temperature and 100 MHz.

Figure 1. ORTEP drawing of **2f**. Thermal ellipsoids are shown at the 30% probability level. Hydrogen atoms are omitted for clarity. Selected bond distances (Å) and angles (deg): Ru1–C1 = 2.410(4), Ru1–C2 = 2.305(5), Ru1–C3 = 2.238(4), Ru1–C4 = 2.438(4), Ru1–C5 = 2.189(4), Ru1–C6 = 2.246(4), Ru1–C9 = 2.210(6), Ru1–C10 = 2.134(6), Ru1–C11 = 2.185(7), Ru1–C12 = 2.188(6), Ru1–C13 = 2.165(5), Ru1–C14 = 2.227(6), C2–C3 = 1.400(6), C5–C6 = 1.416(6), C1–O1 = 1.258(5), C4–O2 = 1.251(5), C1–C2–C3 = 123.3(4), C2–C3–C4 = 121.9(4), C3–C4–C5 = 112.4(4), C4–C5–C6 = 121.6(4), C5–C6–C1 = 123.8(4), C6–C1–C2 = 112.8(4).

of the two carbonyl carbons in **2f** appeared at a higher field (141.3 ppm). The signals for the olefinic carbons of *p*-quinones vary from 68 to 132 ppm depending on their magnetic environment, and most of them are also shifted to higher fields because of π -back-bonding from ruthenium.

The molecular structure of $\text{Ru}(\eta^6\text{-cot})(2,6\text{-dimethoxy-}p\text{-benzoquinone})$ (**2f**) was confirmed by X-ray crystallography, and the ORTEP drawing is shown in Figure 1.

This structure is represented by a highly distorted trigonal bipyramid and is quite similar to that of **1**.²³ Figure 1 shows the η^4 -coordination of the *p*-quinone ligand with olefinic carbons. The axial positions are occupied by an olefinic moiety of 1,3,5-cyclooctatriene

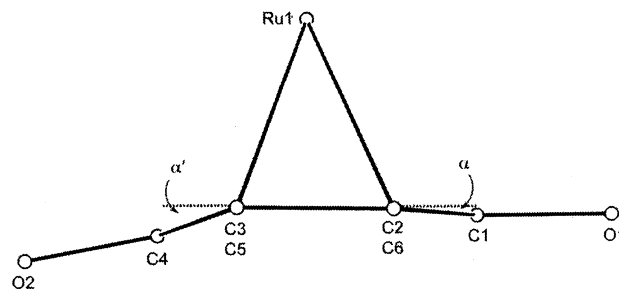


Figure 2. Simplified side view of **2f**. Hydrogen atoms, cyclooctatriene, and two methoxy groups are omitted for clarity. $\alpha = 3.2^\circ$, $\alpha' = 19.0^\circ$.

(C9–C10) and an olefinic moiety of 2,5-dimethoxy-*p*-benzoquinone (C2–C3), which are located diagonally from each other, and other olefinic parts of either cyclooctatriene (C11–C12, C13–C14) or *p*-quinone (C5–C6) are located at the three equatorial positions. The average bond distance between Ru and the four olefinic carbons of *p*-quinone is 2.24 Å. On the other hand, the bond lengths between Ru and the carbonyl carbons of quinone, i.e., Ru–C1 (2.410(4) Å) and Ru–C4 (2.438(4) Å), are longer than the average distance by ca. 0.2 Å. The bond distances of C1–O1 and C4–O2 are 1.258(5) and 1.251(5) Å, respectively, which are typical lengths in transition-metal *p*-quinone complexes.^{5b,14c,15,16,21} A simplified side view of **2f** is shown in Figure 2, where the boat shape of the *p*-quinone ligand can be recognized clearly. The dihedral angles between the plane of four olefinic carbons C2–C3, C5–C6 and the planes that include C1, C2, C6 (α) and C3, C4, C5 (α') are 3.2° and 19.0° , respectively. These angles in transition-metal *p*-quinone complexes are normally $\sim 20^\circ$: for example, $\text{CpRh}(\eta^4\text{-duroquinone})$ (23°),^{5b} $(\pi\text{-C}_9\text{H}_7)\text{Rh}(\eta^4\text{-duroquinone})$ (25°),^{5b} $\text{CpCo}(\eta^4\text{-duroquinone})$ (21°),⁶ and $\text{Cp}^*\text{Ir}(\eta^4\text{-}p\text{-benzoquinone})$ (16°).¹⁵ Since the smallest reported value is 6.0° in $\text{Ni}(\text{cod})(\text{duroquinone})$,⁴ the 3.2° in complex **2f** is quite unusual. Surprisingly, this dihedral angle is even smaller than those of semiquinone complexes such as $\text{Ru}(\eta^6\text{-}p\text{-MeC}_6\text{H}_4\text{SO}_3\text{-H}_2\text{O})(\eta^6\text{-}p\text{-O=C}_6\text{-Me}_4\text{OH})$ (8.7° , 10°)²⁵ and $\text{Mn}(\eta^5\text{-}p\text{-O=C}_6\text{H}_4\text{OH})(\text{CO})_3$ (6.7° , 11.3°).^{19b}

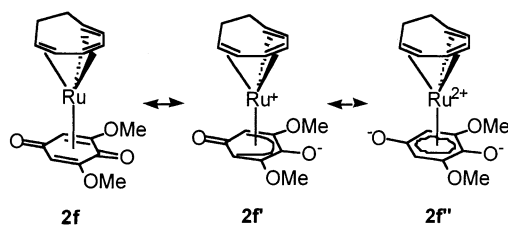
The ambiguity of hapticity is often discussed in transition-metal *p*-quinone complexes.^{11b,19b} Scheme 1 shows possible resonance structures **2f–2f''**. The η^4 -*p*-quinone form (**2f**) basically gives a large contribution because the bond lengths of Ru–C2, C3, C5, C6 are ca. 0.2 Å shorter than those of Ru–C1 and C4. However, the quite small exo-bending ($\alpha = 3.2^\circ$) of the plane that includes C1, C2, and C6 compared to the plane of four

(23) Mitsudo, T.; Suzuki, T.; Zhang, S.-W.; Imai, D.; Fujita, K.; Manabe, T.; Shiotsuki, M.; Watanabe, Y.; Wada, K.; Kondo, T. *J. Am. Chem. Soc.* **1999**, *121*, 1839.

(24) (a) Suzuki, T.; Shiotsuki, M.; Wada, K.; Kondo, T.; Mitsudo, T. *Organometallics* **1999**, *18*, 3671. (b) Suzuki, T.; Shiotsuki, M.; Wada, K.; Kondo, T.; Mitsudo, T. *J. Chem. Soc., Dalton Trans.* **1999**, 4231. (c) Shiotsuki, M.; Suzuki, T.; Kondo, T.; Wada, K.; Mitsudo, T. *Organometallics* **2000**, *19*, 5733.

(25) Koelle, U.; Weisschadel, Chr.; Englert, U. *J. Organomet. Chem.* **1995**, *490*, 101.

Scheme 1. Possible Resonances in 2f



olefinic carbons C2, C3, C5, and C6, as described above, indicates a considerable contribution by an η^5 -*p*-semi-quinone coordination mode (**2f'**). The resonance structure of the hydroquinone dianion (**2f''**) also cannot be ruled out, since the carbonyl carbons of *p*-quinones were shifted upfield by ~ 30 ppm in the ^{13}C NMR spectrum in **2**, as reported for *p*-quinone complexes.^{9,11a,12a,19b} In the infrared spectra of **2**, the $\nu(\text{C}=\text{O})$ bands of the quinone ligands appeared at 1550–1610 cm^{-1} , which are shifted to a lower wavenumber by 50–100 cm^{-1} compared with those of the corresponding free quinones. This shift is attributable to π -back-donation from ruthenium to quinone and also supports some contribution from the structure **2f''**.

Complexes **2** are the first example of zerovalent ruthenium *p*-quinone complexes, whereas Wilkinson and co-workers reported a hydroquinone-bridged divalent ruthenium *p*-quinone complex by reacting $\text{RuH}_2(\text{PPh}_3)_4$ with hydroquinone.¹⁸ Complexes **2** are generally moisture-sensitive due to the highly oxophilic ruthenium center caused by the coordinated *p*-quinones. The reactivity of **2** toward H_2O is dramatically affected by the substituent on the *p*-quinone ligand. For example, complex **2a** was readily decomposed by H_2O in air. On the other hand, complex **2f**, which has two methoxy groups at the 2- and 6-positions, does not react with excess H_2O in dioxane even at a high temperature such as 100 $^\circ\text{C}$.

{Ru(η^6 -cot)}₂(*p*-biquinone) (3**). The reaction of **1** with 0.5 equiv of *p*-biquinone²⁶ in place of *p*-quinone gave a novel Ru(0) bimetallic complex **3** under very mild conditions, as illustrated in eq 1. η^4 -Coordinated monometallic or bimetallic complexes that are similar to complexes **2** did not form at all in this reaction. X-ray crystallography of **3** was successfully performed, and the ORTEP drawing is shown in Figure 3. Symmetrical patterns can be recognized from the top and side views of **3** (Figure 4).**

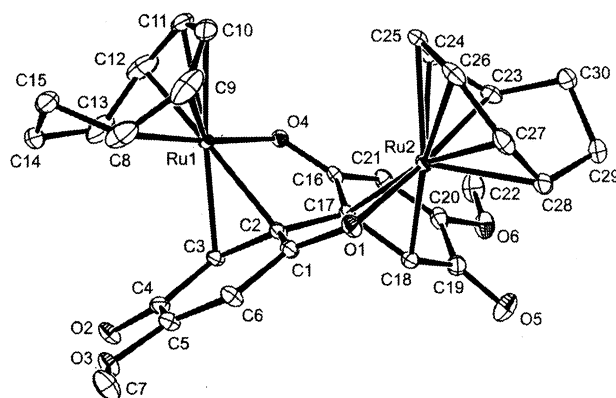
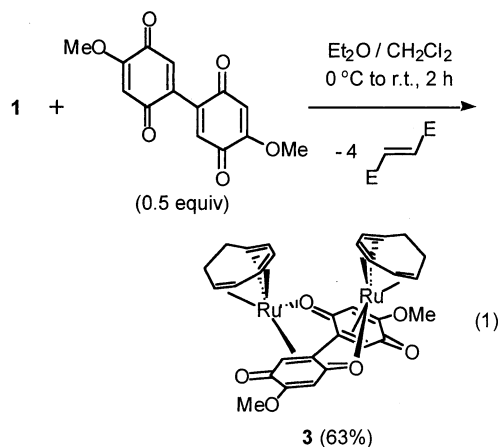


Figure 3. ORTEP drawing of **3**. Thermal ellipsoids are shown at the 30% probability level. Hydrogen atoms are omitted for clarity. Selected bond distances (Å) and angles (deg): Ru1–C2 = 2.152(8), Ru1–C3 = 2.146(7), Ru1–C8 = 2.20(1), Ru1–C9 = 2.12(1), Ru1–C10 = 2.236(9), Ru1–C11 = 2.248(9), Ru1–C12 = 2.18(1), Ru1–C13 = 2.20(1), Ru1–O4 = 2.172(6), C1–C2 = 1.41(1), C2–C3 = 1.46(1), C3–C4 = 1.45(1), C1–O1 = 1.278(9), C2–Ru1–C3 = 39.6(3), C2–Ru1–O4 = 78.3(3), C3–Ru1–O4 = 84.1(3), Ru1–C2–C17 = 105.8(5), Ru1–O4–C16 = 113.6(5), O1–C1–C2 = 120.2(7), C1–C2–C3 = 120.6(7), C2–C3–C4 = 119.6(7), C6–C1–C2 = 120.1(7).

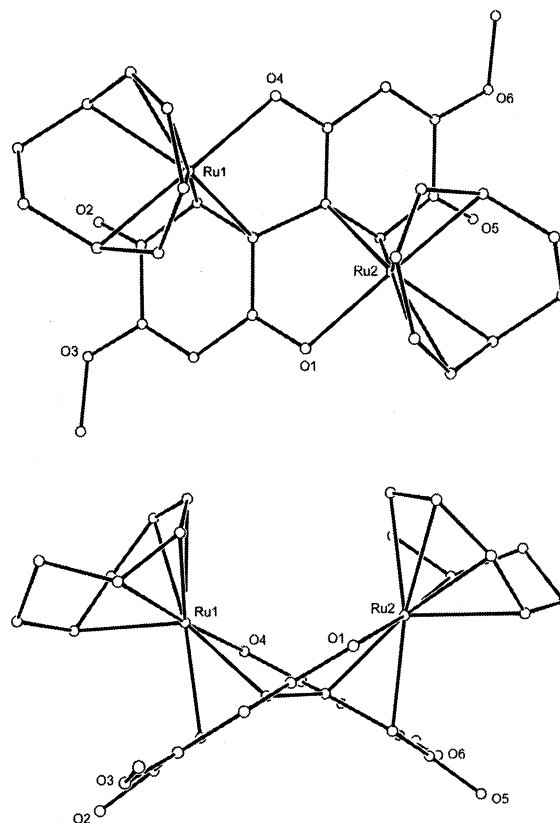


Figure 4. Top and side views of **3**.

In complex **3**, the coordination mode of the *p*-quinone moiety is different from that in **2**. One of the two olefinic parts and an oxygen atom of a carbonyl group of each *p*-quinone moiety coordinate to each ruthenium atom to form stable chelate rings. Two ruthenium atoms are located on the same side of the twisted *p*-biquinone framework. Thus, **3** is a C_2 -symmetric compound and the symmetry axis penetrates the center of *p*-biquinone vertically. The distance between the two ruthenium

atoms is 4.12 Å, and no metal–metal bond exists. The shorter lengths of Ru1–C2 (2.152(8) Å) and Ru1–C3 (2.146(7) Å) and the greater length of C2–C3 (1.46(1) Å) in **3** compared to those in **2f** reveal that the degree of π -back-donation in **3** is much greater than that in **2f**. The C1–O1 bond length in **3** is 1.278(9) Å, which is a little longer than that in **2f**, mainly due to σ -donation from O1 to Ru2. The dihedral angle between a *p*-quinone plane (C1–C6) and a plane containing Ru1, C2, and C3 is 107.7°. Similarly, the dihedral angle between another *p*-quinone plane (C16–C21) and a plane containing Ru2, C17, and C18 is 108.5°. Thus, ruthenium atoms are not located over the hexagonal face of quinones. These quinone planes are twisted relative to each other by 119.1°.

In the ^1H NMR spectrum of **3**, the olefinic protons on C3 and C18 appear at 3.68 ppm, which are considerably shifted to a higher field. A characteristic downfield signal was observed at 202.2 ppm in the ^{13}C NMR, which was assignable to carbonyl carbons C1 and C16. The olefinic carbons of the *p*-biquinone ligand attached to the ruthenium, C2, C17 and C3, C18, appeared at 69.3 and 53.6 ppm, respectively.

A couple of chelations in complex **3** cooperate to strengthen the binding of the *p*-biquinone ligand to each ruthenium atom. An attempt to form a monometallic *p*-biquinone complex by reacting **1** with 1 equiv of *p*-biquinone resulted in failure and gave only the bimetallic complex **3**. This is because the monometallic *p*-biquinone complex can easily capture a second ruthenium by an appropriately located chelation system which was fixed by the first chelation, and as a result, a more stable bimetallic species **3** is formed. Although several transition-metal *p*-quinone complexes have been synthesized so far, such a *p*-biquinone-coordinated bimetallic complex is unprecedented, to the best of our knowledge.

In contrast to the case of complex **1**, reactions of Ru($\eta^4\text{-cod}$)($\eta^6\text{-cot}$) ($\eta^4\text{-cod} = \eta^4\text{-1,5-cyclooctadiene}$), which is a precursor of **1**, with *p*-quinones and *p*-biquinone gave only insoluble materials and did not afford **2** or **3** at all, respectively. This suggests that a π -acidic dimethyl fumarate ligand in **1** is required to control the electron density of ruthenium during substitution by *p*-quinones or *p*-biquinone. In the case of Ru($\eta^4\text{-cod}$)($\eta^6\text{-cot}$), the relatively electron-rich ruthenium center may donate the d-electrons and reduce the coordinated *p*-quinone to a semiquinone anion or a hydroquinone dianion species.

Conclusion

Novel zerovalent ruthenium complexes **2** and **3**, bearing either *p*-quinone or *p*-biquinone as π -acceptors, were synthesized by simple and selective ligand exchange of **1**. Since complexes **2** and **3** are a potentially electron-rich species and also have electron-accepting systems, versatile catalytic activities are expected. Complex **3** has two electron-rich reaction sites located close together without a metal–metal bond, and this unique structure should provide novel catalytic reactions.

Experimental Section

Materials and Methods. All manipulations were performed under an argon atmosphere using standard Schlenk techniques. Ru($\eta^6\text{-cot}$)(dmfm)₂ (**1**) was synthesized as we reported previously.²³ All solvents were distilled under argon over appropriate drying reagents (sodium, calcium hydride, sodium-benzophenone, or calcium chloride). 5,5'-Dimethoxy-2,2'-*p*-biquinone was prepared as reported in the literature.²⁶

Physical and Analytical Measurements. NMR spectra were recorded on JEOL EX-400 (FT, 400 MHz (^1H), 100 MHz (^{13}C)) and AL-300 (FT, 300 MHz (^1H), 75 MHz (^{13}C)) spectrometers. Chemical shift values (δ) for ^1H and ^{13}C are referenced to internal solvent resonances and reported relative to SiMe₄. NMR data for **2a–2g** are summarized in Table 2 (^1H) and Table 3 (^{13}C). IR spectra were recorded on a Nicolet Impact 410 FT-IR spectrometer. Melting points were determined under argon on a Yanagimoto micro melting point apparatus. HR-MS spectra were recorded on JEOL SX102A spectrometers with *m*-nitrobenzyl alcohol (*m*-NBA) as a matrix.

Synthesis of Ru($\eta^6\text{-cot}$)(*p*-quinone), **2a–2g. All of the *p*-quinone complexes **2a–2g** were synthesized in a similar manner. The following procedure for **2a** is representative.**

Ru($\eta^6\text{-cot}$)(*p*-benzoquinone), **2a. A mixture of 100 mg (0.20 mmol) of Ru($\eta^6\text{-cot}$)(dmfm)₂ (**1**), 24 mg (0.22 mmol) of *p*-benzoquinone, and 5 mL of Et₂O was stirred at room temperature for 2 h. The resulting pale yellow precipitate was filtered, rinsed with Et₂O (5 mL \times 5), and dried under vacuum to give the title complex (67 mg, 98%), mp 122 °C (dec). IR (CHCl₃): 1600, 1573 cm⁻¹. HR-MS(FAB-*m*NBA): *m/z* 317.0114 (*M* + *H*)⁺, calcd for C₁₄H₁₅O₂Ru 317.0116.**

Ru($\eta^6\text{-cot}$)(*p*-toluquinone), **2b: pale yellow solid, mp 117 °C (dec). IR (CHCl₃): 1597, 1568 cm⁻¹. HR-MS(FAB-*m*NBA): *m/z* 331.0246 (*M* + *H*)⁺, calcd for C₁₅H₁₇O₂Ru 331.0272.**

Ru($\eta^6\text{-cot}$)(2,6-dimethyl-*p*-benzoquinone), **2c: pale yellow solid, mp 144 °C (dec). IR (KBr disk): 1583, 1558, 1551 cm⁻¹. HR-MS(FAB-*m*NBA): *m/z* 345.0457 (*M* + *H*)⁺, calcd for C₁₆H₁₉O₂Ru 345.0429.**

Ru($\eta^6\text{-cot}$)(2,5-diphenyl-*p*-benzoquinone), **2d: pale yellow solid, mp 233 °C (dec). IR (KBr disk): 1606, 1584 cm⁻¹. HR-MS(FAB-*m*NBA): *m/z* 469.0766 (*M* + *H*)⁺, calcd for C₂₆H₂₃O₂Ru 469.0742.**

Ru($\eta^6\text{-cot}$)(2,5-dichloro-*p*-benzoquinone), **2e: brown solid, mp 221 °C (dec). IR (KBr disk): 1604 cm⁻¹. HR-MS(FAB-*m*NBA): *m/z* 384.9356 (*M* + *H*)⁺, calcd for C₁₄H₁₃Cl₂O₂Ru 384.9336.**

Ru($\eta^6\text{-cot}$)(2,6-dimethoxy-*p*-benzoquinone), **2f: pale yellow solid, mp 172 °C (dec). IR (KBr disk): 1579, 1545 cm⁻¹. HR-MS(FAB-*m*NBA): *m/z* 377.0312 (*M* + *H*)⁺, calcd for C₁₆H₁₉O₄Ru 377.0327.**

Ru($\eta^6\text{-cot}$)(*p*-naphthoquinone), **2g: brown solid, mp 300 °C (dec). IR (Nujol): 1567 cm⁻¹. HR-MS(FAB-*m*NBA): *m/z* 367.0291 (*M* + *H*)⁺, calcd for C₁₈H₁₇O₂Ru 367.0272.**

Synthesis of {Ru($\eta^6\text{-cot}$)}₂(5,5'-dimethoxy-2,2'-*p*-biquinone), **3. To an Et₂O suspension (5 mL) of 5,5'-dimethoxy-2,2'-*p*-biquinone (69 mg, 0.25 mmol) was added a CH₂Cl₂ solution (5 mL) of **1** (248 mg, 0.50 mmol) dropwise at 0 °C. The reaction mixture immediately turned black and was warmed to room temperature. After stirring for 1 h, the solvent was removed, and then CH₂Cl₂ (1.5 mL) and Et₂O (18 mL) were added for recrystallization. The resulting black powder was filtered, washed with Et₂O (3 mL \times 2), and dried under vacuum to give complex **3** (109 mg, 63%), mp 225–227 °C (dec). IR (CHCl₃): 1672, 1621 cm⁻¹. ^1H NMR (400 MHz, CDCl₃): δ 6.66 (dd, *J* = 8.8 and 5.3 Hz, CH of cot, 2H), 6.17 (t, *J* = 8.8 Hz, CH of cot, 2H), 5.52 (m, CH of cot, 2H), 5.25 (s, CH at 6 and 6'-positions of biquinone, 2H), 4.74 (t, *J* = 9.3 Hz, CH of cot, 2H), 4.33 (t, *J* = 6.6 Hz, CH of cot, 2H), 3.68 (s, CH at 3 and 3'-positions of biquinone, 2H), 3.60 (s, OCH₃, 6H), 2.70 (q, *J* = 7.3 Hz, CH of cot, 2H), 2.17 (m, CHH of cot, 2H), 1.64 (m, CHH of cot, 2H), 1.02 (m, CHH of cot, 2H), –0.64 (m, CHH of cot, 2H). ^{13}C NMR**

(26) Jacob, P., III; Callery, P. S.; Shulgin, A. T.; Castagnoli, N., Jr. *J. Org. Chem.* **1976**, *41*, 3627.

Table 4. Summary of Crystal Data, Collection Data, and Refinement of **2f and **3****

	2f	3
formula	C ₁₆ H ₁₈ O ₄ Ru·H ₂ O	C ₃₀ H ₃₀ O ₆ Ru ₂ ·CH ₂ Cl ₂
fw	393.40	773.64
cryst color	yellow	black
habit	prismatic	platelet
cryst size, mm	0.20 × 0.10 × 0.10	0.35 × 0.20 × 0.10
cryst syst	orthorhombic	monoclinic
space group	<i>Pbca</i>	<i>P2₁/n</i>
<i>a</i> , Å	10.5230(3)	10.7583(5)
<i>b</i> , Å	13.5805(3)	23.2869(9)
<i>c</i> , Å	20.7004(5)	11.4630(7)
β , deg		103.372(2)
<i>V</i> , Å ³	2958.2(1)	2793.9(2)
<i>Z</i>	8	4
<i>D</i> (calcd), g cm ⁻³	1.766	1.839
data collection	–50	–130
temp, °C		
μ (Mo K α), cm ⁻¹	10.82	13.18
2θ max, deg	54.9	54.9
no. of measd reflns	28 298	24 764
no. of unique reflns	3371 (<i>R</i> _{int} = 0.057)	6377 (<i>R</i> _{int} = 0.042)
no. of obsd reflns	1948	5076
(<i>I</i> > 3.00 σ (<i>I</i>))		
no. of variables	212	403
<i>R</i> ^a	0.026	0.056
<i>R</i> _w ^a	0.030	0.073
GOF	0.43	1.61

$$^a R = \sum ||F_o| - |F_c|| / \sum |F_o|; R_w = [\sum w(|F_o| - |F_c|)^2 / \sum w F_o^2]^{1/2}.$$

(100 MHz, CDCl₃): δ 202.2, 191.4, 161.9, 105.9, 105.0, 101.6, 92.2, 87.0, 86.2, 69.3, 66.0, 56.4, 53.6, 33.2, 25.3. HR-MS(FAB-*m*NBA): *m/z* 690.0134 (M)⁺, calcd for C₃₀H₃₀O₆Ru₂ 690.0129.

Crystallographic Study of Complexes **2f and **3**.** Single crystals of complexes **2f** and **3** obtained by recrystallization from CHCl₃/pentane (**2f**) or CH₂Cl₂/pentane (**3**) were subjected to X-ray crystallographic analysis. The crystal data and experimental details for **2f** and **3** are summarized in Table 4. All measurements were made on a Rigaku RAXIS imaging plate area detector with graphite-monochromated Mo K α

radiation (λ = 0.71069 Å). The structures were solved by direct methods using SIR92²⁷ and expanded using Fourier techniques, DIRDIF99.²⁸ The non-hydrogen atoms were refined anisotropically, except for an oxygen atom of a lattice water in **2f**, which was refined isotropically. Hydrogen atoms were refined using the riding model. Neutral atom-scattering factors were taken from Cromer and Waber.²⁹ Anomalous dispersion effects were included in *F*_{calc},³⁰ the values for $\Delta f'$ and $\Delta f''$ were those of Creagh and McAuley.³¹ The values for the mass attenuation coefficients were those of Creagh and Hubbell.³² All calculations were performed using the CrystalStructure^{33,34} crystallographic software package.

Acknowledgment. This work was supported in part by Grants-in-Aid for Scientific Research from the Ministry of Education, Science, Sports and Culture, Japan.

Supporting Information Available: Description of the X-ray procedures, tables of X-ray data, positional and thermal parameters, and bond lengths and angles, and an ORTEP diagram for compounds **2f** and **3**. This material is available free of charge via the Internet at <http://pubs.acs.org>.

OM020730A

(27) Altomare, A.; Cascarano, G.; Giacovazzo, C.; Guagliardi, A.; Burla, M.; Polidori, G.; Camalli, M. *J. Appl. Crystallogr.* **1994**, *27*, 435.

(28) Beurskens, P. T.; Admiraal, G.; Beurskens, G.; Bosman, W. P.; de Gelder, R.; Israel, R.; Smits, J. M. M. *The DIRDIF-99 program system*; Technical Report of the Crystallography Laboratory: University of Nijmegen, Netherlands, 1999.

(29) Cromer, D. T.; Waber, J. T. *International Tables for X-ray Crystallography*; The Kynoch Press: Birmingham, England, Vol. IV, 1974.

(30) Ibers, J. A.; Hamilton, W. C. *Acta Crystallogr.* **1964**, *17*, 781.

(31) Creagh, D. C.; McAuley, W. J. *International Tables for X-ray Crystallography*; Kluwer Academic Publishers: Boston, Vol. C, 1992.

(32) Creagh, D. C.; Hubbell, J. H. *International Tables for X-ray Crystallography*; Kluwer Academic Publishers: Boston, Vol. C, 1992.

(33) *CrystalStructure 2.00, Crystal Structure Analysis Package*; Rigaku and MSC, 2001.

(34) Watkin, D. J.; Prout, C. K.; Carruthers, J. R.; Betteridge, P. W. *CRYSTALS Issue 10*; Chemical Crystallography Laboratory: Oxford, UK.